

The Nucleon Polarizability Program at MAMI-A2

GARTH HUBER¹

*Department of Physics
University of Regina, Regina, SK S4S-0A2 CANADA*

CRISTINA COLLICOTT

*Department of Physics and Atmospheric Science
Dalhousie University, Halifax, NS B3H-4R2 CANADA*

ON BEHALF OF THE A2 COLLABORATION

Low energy Compton scattering allows the investigation of one of the fundamental properties of the nucleon – how its internal structure deforms under an applied electromagnetic field. We review recent developments in the investigation of proton polarizabilities, and our plans for future measurement at the Mainz Microtron (MAMI).

PRESENTED AT

Conference on the Intersections of
Particle and Nuclear Physics (CIPANP)
Vail, CO USA May 19–24, 2015

¹Work supported by the Natural Sciences and Engineering Research Council of Canada (NSERC); FRN: 105851-2011 and SAPPJ-2015-00023.

1 Introduction to Polarizabilities

Nucleon polarizabilities are fundamental structure properties which are sensitive to the internal quark dynamics of the nucleon. They can be accessed by measuring the differential cross section and singly and doubly polarized asymmetries in Real Compton Scattering. In this case, the low energy outgoing Compton photon plays the role of the applied electromagnetic dipole field. In addition to their obvious interest as nucleon structure observables, nucleon polarizabilities limit the precision that can be accessed in many other areas of physics. For example, in astrophysics, the polarizabilities influence the properties of neutron stars. In atomic physics, the polarizabilities yield an appreciable correction to Lamb shift and hyperfine structure. In fact, the uncertainty in the proton's scalar polarizability is the largest uncertainty in the proton radius extraction from the atomic hydrogen excitation spectrum [1].

The proton's electric and magnetic polarizabilities appear in the second order term in the Compton scattering Hamiltonian

$$H_{eff}^{(2)} = \frac{1}{2}\alpha_{E1}\vec{E}^2 + \frac{1}{2}\beta_{M1}\vec{H}^2, \quad (1)$$

where $\alpha_{E1} = (11.2 \pm 0.4) \times 10^{-4} \text{ fm}^3$ and $\beta_{M1} = (2.5 \pm 0.4) \times 10^{-4} \text{ fm}^3$ [2]. Despite their all-pervading nature, and great theoretical interest, there is still a large uncertainty in the nucleon scalar polarizabilities. α_{E1} is well constrained by experimental data, but β_{M1} is less certain, and the neutron data are particularly uncertain.

The spin polarizabilities appear in the third order term of the effective interaction Hamiltonian

$$H_{eff}^{(3)} = \frac{1}{2}[\gamma_{E1E1}\vec{\sigma} \cdot \vec{E} \times \dot{\vec{E}} + \gamma_{M1M1}\vec{\sigma} \cdot \vec{H} \times \dot{\vec{H}} + 2\gamma_{E1M2}H_{ij}\sigma_i E_j - 2\gamma_{M1E2}E_{ij}\sigma_i H_j], \quad (2)$$

involving one field derivative with respect to either time or space $\dot{\vec{E}} = \partial_t \vec{E}$, $E_{ij} = 1/2(\nabla_i E_j + \nabla_j E_i)$. For example, γ_{M1E2} represents the contribution where the proton is excited by electric quadrupole ($E2$) radiation and decays by magnetic dipole ($M1$) radiation. The spin polarizabilities describe the ‘‘stiffness’’ of the proton's spin against electromagnetic-induced deformations relative to the spin axis, defining the frequency of the proton's spin precession induced by variable electromagnetic fields. Each spin polarizability is dominated by a pion-pole contribution, the dispersive (interesting) contribution is expected to be relatively small.

The proton's spin polarizabilities have never been measured, although the forward and backward linear combinations γ_0 and γ_π have been. The forward spin polarizability $\gamma_0 = -\gamma_{E1E1} - \gamma_{M1M1} - \gamma_{E1M2} - \gamma_{M1E2}$ can be obtained from the polarized Compton cross section difference $\sigma_{1/2} - \sigma_{3/2}$. It is known to about 10%, $\gamma_0 = -(1.00 \pm 0.08 \pm 0.10) \times 10^{-4} \text{ fm}^4$ [3] and the pole contribution is believed to cancel. The backward spin polarizability $\gamma_\pi = \gamma_{E1E1} + \gamma_{M1M1} - \gamma_{E1M2} + \gamma_{M1E2}$ is

obtained from unpolarized backward angle Compton scattering, and a recent analysis gives the value as $\gamma_\pi = -(38.7 \pm 1.8) \times 10^{-4} \text{ fm}^4$ [4]. The pion contribution has been calculated as -46.7, so the dispersive part 8.0 ± 1.8 is known only to about 25%.

2 Measurements by A2 Collaboration at MAMI

The polarizability program at MAMI is very active, with developments in equipment, experiment and theory. These are intended to produce a comprehensive, consistent and precise data set, necessary for a reliable extraction of the scalar polarizabilities of the proton and the neutron, and the world's first independent extraction of the proton spin polarizabilities. The A2 Collaboration utilizes a high-flux tagged bremsstrahlung photon beam, liquid hydrogen or dynamically polarized butanol frozen spin target, and the large acceptance Crystal Ball and TAPS detectors for these measurements. For more information, see Ref. [5].

Until now, experiments relying on Dispersion Relation (DR) analysis have only been able to extract the sum and difference of α_{E1} , β_{M1} , resulting in correlated errors for the two quantities, and since the magnetic polarizability is much smaller than the electric, the relative error on β_{M1} is large. The desire for more precise proton β_{M1} has motivated a next generation experiment at MAMI-A2. If combinations of cross sections with *linearly polarized photon beam* are used, the leading-order contributions from α_{E1} , β_{M1} are [6]

$$\begin{aligned} \frac{d\sigma^\parallel}{d\Omega} &= \frac{d\sigma_{Powell}^\parallel}{d\Omega} - \frac{e^2}{2\pi m_p} \left(\frac{\nu'}{\nu}\right)^2 \nu\nu'(\alpha_{E1} \cos^2 \theta + \beta_{M1} \cos \theta) + O(\nu^3) \\ \frac{d\sigma^\perp}{d\Omega} &= \frac{d\sigma_{Powell}^\perp}{d\Omega} - \frac{e^2}{2\pi m_p} \left(\frac{\nu'}{\nu}\right)^2 \nu\nu'(\alpha_{E1} + \beta_{M1} \cos \theta) + O(\nu^3). \end{aligned} \quad (3)$$

Thus, the contributions of the two scalar polarizabilities can in principle be disentangled from measurements of the Compton angular distribution with linearly polarized photon beam. More recently, Krupina and Pascalutsa [7] have shown that for energies below the Δ resonance, it is better to use the polarized beam asymmetry Σ_3 to extract the poorly-known β_{M1}

$$\Sigma_3 \equiv \frac{d\sigma^\perp - d\sigma^\parallel}{d\sigma^\perp + d\sigma^\parallel} = \Sigma_3^{Born} - f_3(\theta)\beta_{M1}\nu^2 + O(\nu^4). \quad (4)$$

Following this motivation, we recently measured, for the first time, the beam asymmetry Σ_3 below pion production threshold ($E_\gamma = 80 - 140 \text{ MeV}$). More than 70.000 $\gamma p \rightarrow \gamma p$ events for each of the two polarization settings were obtained, with an overall background contamination below 5%. The preliminary data are in a good agreement with Chiral Perturbation Theory (χ PT) [7] and Heavy Baryon Chiral

Perturbation Theory (HB χ PT) [8] calculations, however, a noticeable deviation from the Born term, independent of proton polarizabilities (see Eqn. 4) was observed. The data will be presented, along with the corresponding estimates for the proton scalar polarizabilities, in an upcoming publication [9]. So far, only 1/3 of the approved data were taken. The remaining 2/3 of the data are expected to be acquired in 2016, after an upgrade of the Glasgow-Mainz tagger to allow four times higher rate compared to the already performed measurement.

Since the spin polarizabilities appear in the effective interaction Hamiltonian at third order in photon energy, they are a small effect at lower energies. It is in the Δ resonance region ($E_\gamma = 200 - 300$ MeV) where their effect becomes significant. In this energy region, it is possible to accurately measure polarization asymmetries using a variety of polarized beam and target combinations. The various asymmetries respond differently to the individual spin polarizabilities at different E_γ and θ , so it is by measuring at least three different asymmetries at different E_γ , θ that their contributions can be isolated. The plan of the A2 Collaboration is to conduct a global analysis, including constraints from all available prior data (e.g. α_{E1} , β_{M1} , γ_0 , γ_π) to independently extract all four spin polarizabilities with small statistical, systematic and model-dependent errors.

The Σ_3 single-spin asymmetry with linearly polarized beam has been defined above. The two double-spin asymmetries of interest with circularly polarized beam are defined as

$$\Sigma_{2z} = \frac{\left(\frac{d\sigma}{d\Omega}\right)_{\uparrow\uparrow} - \left(\frac{d\sigma}{d\Omega}\right)_{\uparrow\downarrow}}{\left(\frac{d\sigma}{d\Omega}\right)_{\uparrow\uparrow} + \left(\frac{d\sigma}{d\Omega}\right)_{\uparrow\downarrow}}, \quad \Sigma_{2x} = \frac{\left(\frac{d\sigma}{d\Omega}\right)_{\uparrow\rightarrow} - \left(\frac{d\sigma}{d\Omega}\right)_{\uparrow\leftarrow}}{\left(\frac{d\sigma}{d\Omega}\right)_{\uparrow\rightarrow} + \left(\frac{d\sigma}{d\Omega}\right)_{\uparrow\leftarrow}}, \quad (5)$$

where the second $\uparrow\downarrow$ indicate transversely polarized nucleon target orientation, and the \rightarrow indicate longitudinally polarized target.

These measurements are quite challenging. The Compton scattering cross section is small, only about 1% of the dominant π^0 photoproduction process at these energies, and under certain conditions π^0 photoproduction can mimic the Compton scattering signature if one of the photons escapes the detector or if the electromagnetic showers from the two photons overlap (due to finite angular resolution). In addition, coherent and incoherent reactions from C, O, He in the polarized butanol target need to be identified and subtracted. In the Δ -region, the use of the recoil proton track can sometimes assist in the suppression of non-Compton backgrounds, but the energy losses in the target elements and inner detector elements are considerable and greatly restrict the kinematic region where the recoil proton track provides reliable information.

Fig. 1 provides an example of these background contributions from our recent Σ_{2x} analysis [10]. After the indicated cuts are applied, a clean data sample is obtained. Our first measurement of a double-spin Compton scattering asymmetry on the nucleon is shown in Fig. 2. As indicated, the results are clearly sensitive to the value of γ_{E1E1}

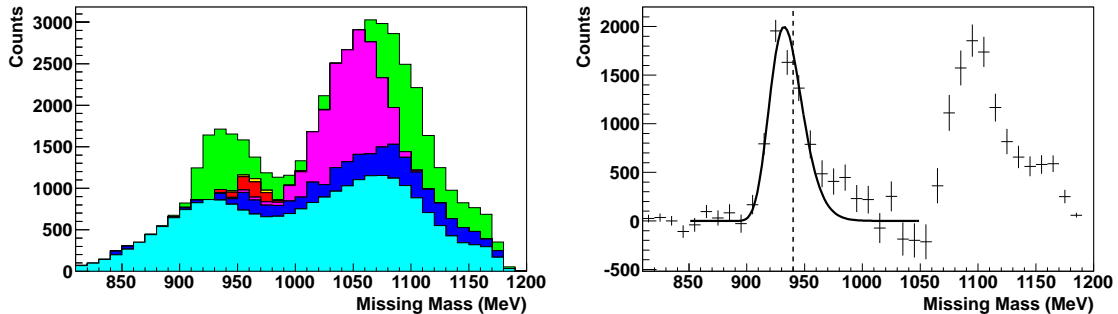


Figure 1: **Left:** Data Missing Mass distribution from Σ_{2x} analysis for $E_\gamma = 273 - 303$ MeV, $\theta_{LAB}^\gamma = 100 - 120^\circ$ [10] (green) with various background contributions indicated as follows: accidental coincidences (cyan), carbon/cryostat contributions (blue), reconstructed π^0 background where one decay γ escapes the setup via the TAPS downstream hole (red), or the Crystal Ball upstream hole (magenta). **Right:** Fully-subtracted Missing Mass spectrum with simulated Compton peak overlaid. A conservative $MM < 940$ MeV cut is then applied to exclude π^0 production.

in the calculation, but not very sensitive to the value of γ_{M1M1} . Additional data to further reduce the Σ_{2x} error bars are planned to be acquired in 2017.

In Fig. 3 are our preliminary results for Σ_3 in the resonance region [12]. Similar to Fig. 1, restrictive cuts to eliminate π^0 and other backgrounds are applied, resulting in a clean data sample. The resulting missing mass distribution agrees well with our Compton scattering simulations, and the extracted Σ_3 for π^0 photoproduction also agrees well with previously published data. Our Σ_3 results are also compared to those from the LEGS Collaboration [13] in Fig. 3. Even though the statistical uncertainties from both measurements are rather large, a shift in the asymmetries can be observed, particularly near 90° in the higher energy region. The MAMI results suggest that the Σ_3 asymmetry may fall off more rapidly than predicted at backward angles.

A recent analysis by Martel, et al. [10] determined the proton's spin polarizabilities for the first time, combining Σ_3 results from the LEGS Collaboration [13] and Σ_{2x} results from MAMI. The analysis used a fixed- t DR code, provided by B. Pasquini [11], to fit the asymmetry data. The fitting routine varies $\alpha + \beta$, $\alpha - \beta$, γ_0 , γ_π and γ_{E1E1} , γ_{M1M1} , to fit the asymmetry data. The first four are allowed to vary only within their known experimental uncertainties. These results are shown in the third column of Table 1.

The LEGS cross section data have some significant discrepancies when compared to other data sets [15]. Because it is possible that a discrepancy exists only in the cross sections and not the asymmetries, it is worthwhile to check the sensitivity of the extracted spin polarizability results to these data. In this case, the same fitting algorithm applied in the Martel, et al. [10] analysis was applied also to the new

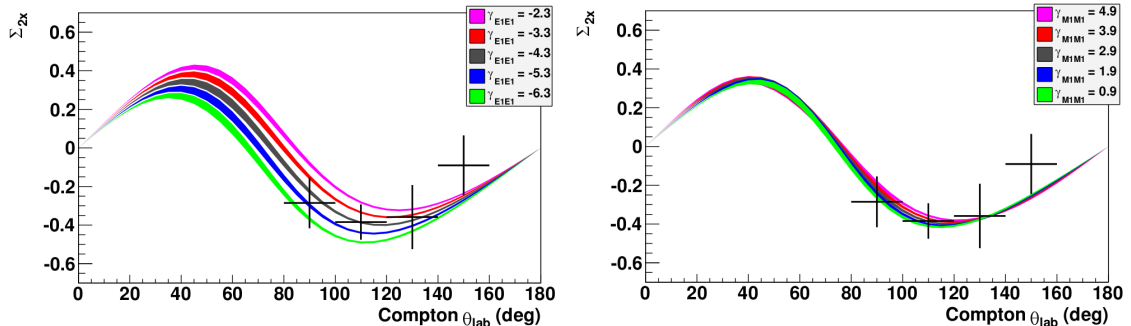


Figure 2: Σ_{2x} results for $E_\gamma = 273 - 303$ MeV versus θ_{LAB}^γ [10]. Overlaid are DR calculations of Pasquini et al. [11] making use constraints on $\alpha_{E1} + \beta_{M1}$, $\alpha_{E1} - \beta_{M1}$, γ_0 , γ_π (allowed to vary within experimental errors). **Left:** γ_{M1M1} is fixed in the calculation and γ_{E1E1} is varied, as indicated. **Right:** γ_{E1E1} is fixed and γ_{M1M1} is varied.

MAMI Σ_3 results, resulting in the values shown in the fourth column of Table 1. This is the first extraction of all four spin polarizabilities using only MAMI data.

It is important to note that the LEGS Σ_3 data set covers a wide angular and energy range and consists of 58 data points, while the MAMI Σ_3 data are only 12 data points. A comparison of the two sets of γ_i values show that the errors on the individual spin polarizabilities increase slightly when using only MAMI data. However, considering the reduced data set in comparison to LEGS, this is to be expected. While the value of γ_{M1M1} remains nearly unchanged, a significant shift is seen in the other three spin polarizabilities. Note in particular the significant shift in γ_π . It has been noted previously [15] that the LEGS data show a large discrepancy from all other data sets when used to extract γ_π . This discrepancy is further confirmed here. Because γ_{E1M2} and γ_{M1E2} are determined through their linear relation to γ_0 , γ_π , a large shift in γ_π helps to explain the differing spin polarizabilities.

In summary, the polarizabilities program at MAMI is very active, providing new data for testing QCD via Chiral Perturbation Theory and Dispersion Relations in the non-perturbative regime. For the scalar polarizabilities, we have demonstrated a new technique to extract β_{M1} from the Σ_3 asymmetry without correlated errors to the larger α_{E1} . Additional data to complete this measurement are planned for 2016. Regarding the spin polarizabilities, we have embarked on a three part program to extract all four spin polarizabilities independently with small statistical, systematic and model-dependent errors. We have measured the Σ_{2x} double-spin asymmetry for the first time, and plan to acquire additional statistics in the next 2 years. We have taken new Σ_3 data to supplement existing data, and used both asymmetries to extract the four spin polarizabilities for the first time. Our planned Σ_{2z} data will further constrain the spin polarizabilities. The first set of these data were acquired

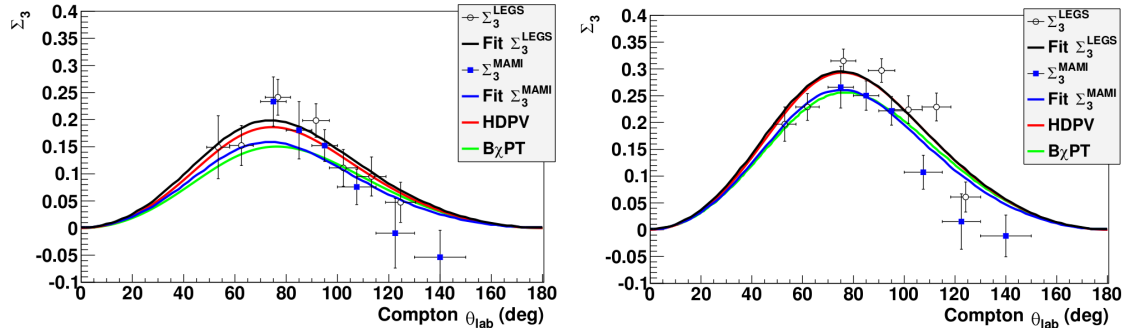


Figure 3: Preliminary Σ_3 results for **Left:** $E_\gamma = 267 - 287$ MeV, **Right:** $E_\gamma = 287 - 307$ MeV, versus θ_{LAB}^γ [12], in comparison with previously published data from LEGS [13]. Overlaid are DR calculations of Refs. [11, 14] using their preferred polarizabilities. Only statistical uncertainties are shown.

in 2014, and we have just concluded a very successful second run in the summer of 2015. Finally, the A2 Collaboration plans to eventually extend the polarizability measurements to the neutron, using a high-pressure active ^3He gas scintillator target [16].

ACKNOWLEDGEMENTS

We wish to thank the MAMI accelerator group and staff for their outstanding support, and the CIPANP conference organizers for the talk invitation.

References

- [1] I.B. Khriplovich, R.A. Sen'kov, Phys. Lett. A **279**, 474 (1998).
- [2] K.A. Olive, et al. (Particle Data Group), Chin. Phys. C **38**, 090001 (2014).
- [3] J. Ahrens, et al. (GDH and A2 Collaborations), Phys. Rev. Lett. **87**, 022003 (2001).
- [4] M. Schumacher, Prog. Part. Nucl. Phys. **55**, 567 (2005).
- [5] A. Neiser (A2 Collaboration), J. Phys. Conf. Ser. **587**, 012041 (2015).
- [6] L.C. Maximon, Phys. Rev. C **39**, 347 (1989)
- [7] N. Krupina, V. Pascalutsa, Phys. Rev. Lett. **110**, 262011 (2013).

	HDPV [11]	B χ PT [14]	Σ_{2x} and Σ_3^{LEGS} [10]	Σ_{2x} and Σ_3^{MAMI} [12]
γ_{E1E1}	-4.3	-3.3	-3.5 ± 1.2	-5.0 ± 1.5
γ_{M1M1}	2.9	3.0	3.16 ± 0.85	3.13 ± 0.88
γ_{E1M2}	-0.0	0.2	-0.7 ± 1.2	1.7 ± 1.7
γ_{M1E2}	2.2	1.1	2.0 ± 0.3	1.3 ± 0.4
γ_0	-0.8	-1.0	-1.03 ± 0.18	-1.00 ± 0.18
γ_π	9.4	7.2	9.3 ± 1.6	7.8 ± 1.8
$\alpha + \beta$			14.0 ± 0.4	13.8 ± 0.4
$\alpha - \beta$			7.4 ± 0.9	6.6 ± 1.7
$\chi^2/d.f.$			1.05	1.25

Table 1: Dispersion Relation fits to Σ_{2x} along with either Σ_3^{LEGS} or Σ_3^{MAMI} . Also shown are the preferred values from two models. Spin polarizabilities are in units of 10^{-4} fm^4 , and scalar polarizabilities are in units of 10^{-4} fm^3 .

- [8] J. McGovern, D. Phillips, H. Griesshammer, Eur. Phys. J. A **49**, 12 (2013).
- [9] V. Sokhoyan, et al. (A2 Collaboration), to appear.
- [10] P. Martel, et al. (A2 Collaboration), Phys. Rev. Lett. **114**, 112501 (2015), arXiv:1408.1576.
- [11] B. Pasquini, et al., Phys. Rev. C **76**, 014203 (2007).
- [12] C. Collicott, et al. (A2 Collaboration), to appear.
C. Collicott, Ph.D. thesis, Dalhousie University, 2015.
<http://dalspace.library.dal.ca/handle/10222/56762>
- [13] G. Blanpied, et al. (LEGS Collaboration), Phys. Rev. C **64** 025203 (2001).
- [14] V. Lensky, J. McGovern, Phys. Rev. C **89** 032202 (2014).
- [15] M. Camen, et al., Phys. Rev. C **65**, 032202(R) (2002).
- [16] J. Annand, et al. (A2 Collaboration), MAMI Proposal A2-01-2013.